CREEP FRACTURE OF CERAMIC-MATRIX COMPOSITES

B. Wilshire and H. Burt

Department of Materials Engineering, University of Wales,
Swansea, SA2 8PP, UK

ABSTRACT

The tensile creep and creep fracture properties in air at 1573K are compared for four composites produced with Al_2O_3 or SiC matrices, reinforced with interwoven bundles of either Nicalon™ or Hi-Nicalon™ fibres aligned at 0/90° to the stress axis. This analysis identifies the creep damage processes governing the strains and times to failure, suggesting avenues for development of improved SiC-fibre-reinforced ceramic-matrix materials.

KEYWORDS

Creep; Creep Fracture; Ceramic-Matrix Composites; Fibre Reinforcement.

INTRODUCTION

To combat the toughness deficiencies of monolithic ceramics, major R&D programmes have been directed to the manufacture and evaluation of ceramic-matrix composites (CMCs) reinforced with dispersions of ceramic whiskers or with arrays of ceramic fibres. However, for applications involving long periods of service without failure under load at high temperatures, fibre-reinforced CMCs display creep and creep fracture properties which are superior to those exhibited by whisker-reinforced products [1]. In seeking to interpret the creep behaviour patterns observed for fibre-reinforced composites, the damage processes leading to fracture have often been inferred [2-6] from the creep mismatch ratio (CMR) defined [2] as

$$CMR = \dot{\varepsilon}_F / \dot{\varepsilon}_M \qquad (1)$$

where $\dot{\varepsilon}_F$ and $\dot{\varepsilon}_M$ are the creep rates of the fibres and matrices respectively. With this concept [2], when the creep resistance of the fibres exceeds that of the matrix (CMR < 1), the dominant damage mechanism is considered to be periodic fibre failure. Conversely, when the fibres have a lower creep strength than the matrix (CMR > 1), the principal damage process is seen as matrix cracking. Yet, even for nominally-identical fibre-reinforced materials, the fibres have been considered to be more creep resistant than the matrix [7] and *vice versa* [4]. For this reason, the comparative creep strengths of the fibres and the matrices are now assessed for a series of fibre-reinforced CMCs, anticipating that the mechanistic insights gained by understanding the processes governing creep damage accumulation and fracture will indicate practical avenues for development of improved product ranges.

MATERIALS

The strength characteristics of fibre-reinforced CMCs depend on load transfer to large volume fractions of high-modulus fibres, with weak fibre-matrix interfaces allowing intact fibres to bridge across the faces of cracks developing in the ceramic matrices [8-10]. To clarify the rôles of the fibres, matrices and fibre/matrix interfaces in determining the creep and creep fracture properties, the present study considers four CMCs, reinforced with various types of silicon carbide fibres, namely,

- a SiC-fibre-reinforced Al_2O_3-matrix composite [7], designated as SiC_f/Al_2O_3, and
- three SiC-fibre-reinforced SiC-matrix materials, now referred to as standard SiC_f/SiC [7], enhanced SiC_f/SiC [5] and $HNSiC_f/SiC$ [6].

The distinguishing compositional and microstructural characteristics of these four composites are summarized in Table 1, with the following comments made to amplify the descriptions given.

All materials were reinforced with ~0.4 volume fractions of ~12 to 15μm diameter SiC fibres, incorporated as bundles of ~500 fibres interwoven to form 2D layers of fabric, which were aligned and stacked to obtain multilayer samples having 0/90° fibre architectures. However, the standard SiC_f/SiC and enhanced SiC_f/SiC specimens were produced with plain woven bundle configurations, while the $HNSiC_f/SiC$ and SiC_f/Al_2O_3 were made with a satin weave. Compared with the plain woven arrays, the extent to which the fibres bend under load and the attendant risk of fibre damage should be lower with the satin weave.

In addition to differences in weave pattern, these 0/90° composites were reinforced with two types of SiC fibre. Thus, the SiC_f/Al_2O_3, standard SiC_f/SiC and enhanced SiC_f/SiC samples were produced using Nicalon™ NLM 202 fibres (Nippon Carbon Co., Tokyo, Japan). With these fibres, the presence of an amorphous oxycarbide ($SiC_{0.85}O_{0.15}$) phase results in a loss of creep resistance during long term exposure at elevated temperatures [11]. This deleterious amorphous phase can be eliminated by electron radiation under vacuum [12,13], giving the Hi-Nicalon™ fibre used to reinforce the $HNSiC_f/SiC$ product (Table 1). As well as possessing a higher modulus, these Hi-Nicalon™ fibres are expected to display better long-term creep strengths than Nicalon™ NLM 202 fibres.

The fibres in the SiC_f/Al_2O_3 material were coated with a thin BN layer before a ~5μm thick SiC coating was deposited by chemical vapour infiltration (CVI). The Al_2O_3 matrix was then introduced by *in-situ* directional oxidation of a liquid aluminium [14,15]. In contrast, with the three SiC-fibre-reinforced SiC-matrix composites (now collectively termed SiC_f/SiC type materials), thin carbon interface layers were obtained by decomposition of a hydrocarbon gas before the fibre preforms were CVI densified to produce the SiC matrices. Although the methods used to create the ceramic matrices were different, in all cases, the matrix porosities were ~15%.

Compared with the double BN/SiC interfaces in the SiC_f/Al_2O_3 samples, the carbon interfaces in the SiC_f/SiC type materials are more prone to oxidation during creep exposure. For this reason, the SiC matrices in the enhanced SiC_f/SiC and $HNSiC_f/SiC$ products contained boron-based particulate additives. These additives react with oxygen to form a borosilicate glass, which seals cracks developing in the 'enhanced' matrices [16,17]. In this way, the vulnerable carbon interfaces are protected by limiting oxygen penetration into the testpieces during creep.

TABLE 1

DISTINGUISHING CHARACTERISTICS OF THE SiC FIBRE-REINFORCED COMPOSITES

| MATERIAL DESIGNATION	FIBRE TYPE	INTERFACE TYPE and THICKNESS	MATRIX TYPE	REF
SiC_f/Al_2O_3	Nicalon™ NLM 202	BN/SiC (~5μm)	Al_2O_3	7
Standard SiC_f/SiC	Nicalon™ NLM 202	Carbon (<0.5μm)	SiC	7
Enhanced SiC_f/SiC	Nicalon™ NLM 202	Carbon (<0.5μm)	Enhanced SiC	5
$HNSiC_f/SiC$	Hi- Nicalon™	Carbon (<0.5μm)	Enhanced SiC	6

RESULTS and DISCUSSION

The creep and creep fracture properties of the 0/90° fibre-reinforced CMCs (Table 1) can be compared using data obtained in tensile creep tests carried out in air at 1573K [5-7]. Under the test conditions studied, continuously decaying creep curves were recorded, i.e. after the initial strain on loading at the creep temperature, the creep rate decreased gradually with time towards a minimum value, with no well-defined secondary or tertiary creep stages apparent before fracture occurred. However, with the standard SiC_f/SiC samples, the creep strains to failure were low (~0.002) at all stress levels [7]. In contrast, with the other three materials, the creep ductility appeared to increase with decreasing stress, approaching values of ~0.03 in tests of around 3000 hours duration with the SiC_f/Al_2O_3 specimens [7].

Fibre Control of Creep and Fracture

At 1573K, the UTS for the SiC_f/Al_2O_3 samples is the same as the value (~230 MPa) recorded for the three SiC_f/SiC type products [5,6]. Moreover, broadly similar stress/minimum creep rate behaviour is found for all four CMCs (Figure 1a). Clearly, stresses about five times larger must be applied to Nicalon™ NLM 202 fibres [18] to achieve creep rates comparable with those observed for the Nicalon™-fibre-reinforced materials. Since the longitudinal (0°) fibres occupy about one fifth of the crosssectional areas of the testpieces, for all four 0/90° composites, the creep strength is determined by the longitudinal fibres.

Although the fibre reinforcements are similar for the four CMCs (Table 1), the creep and creep rupture strengths are comparable for the SiC_f/Al_2O_3, the enhanced SiC_f/SiC and the $HNSiC_f/SiC$ samples, but inferior properties are displayed by the standard SiC_f/SiC material (Figure 1). This seemingly-anomalous result is attributable to differences in creep ductility [7]. Thus, when continuously-decaying creep curves are observed in tension, the rupture life (t_f) can be defined as the time taken for the accumulated creep strain to reach the limiting creep ductility (ε_f). Simultaneously, the creep rate decays with time, reaching the minimum creep rate ($\dot{\varepsilon}_m$) as the curves terminate. The creep curves presented in Figure 2 then show that the initial variations in creep strain with time are similar for the standard SiC_f/SiC and enhanced SiC_f/SiC products, as would be expected for two materials having nominally-identical fibre reinforcement (Table 1). However, low ductility termination of the creep curves for the standard SiC_f/SiC samples (Figure 2) leads to minimum creep rates which are faster and rupture lives which are shorter than the values found when failure occurs at higher ductilities with the other three composites. (Figures 1 and 2).
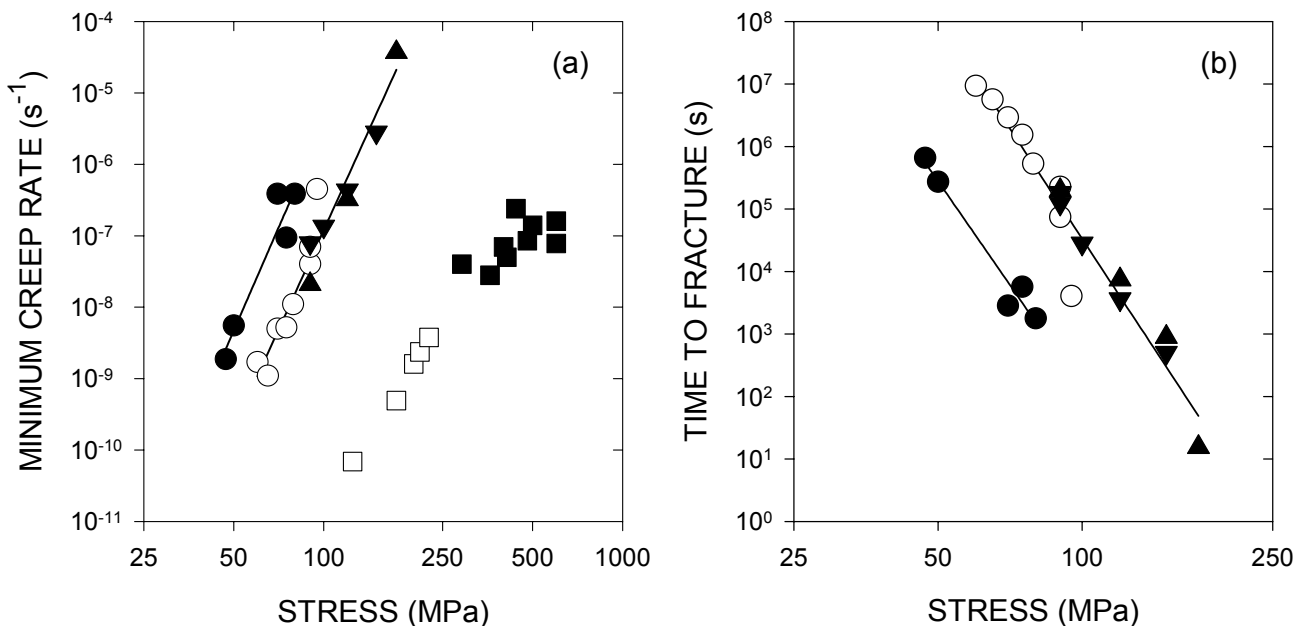

Figure 1. Variations of (a) minimum creep rate and (b) creep rupture life with stress for SiC_f/Al_2O_3 [○], standard SiC_f/SiC [●], enhanced SiC_f/SiC [▲] and $HNSiC_f/SiC$ [▼] composites at 1573K, together with creep data for Nicalon™ NLM 202 fibres [■] at 1573K and sintered silicon carbide [□] at 1773K.

Oxidation Effects During Creep

Since the creep ductility defines the point of creep curve termination (Figure 2), thereby affecting the minimum creep rates and rupture lives recorded (Figure 1), it is necessary to explain ductility variations in relation to the damage processes leading to fracture. For all CMCs considered (Table 1), the rates of creep strain accumulation are determined by the creep resistance of the longitudinal fibres, with creep of the fibres accompanied by cracking of the weak brittle matrices (Figure 3a). The developing matrix cracks can by-pass transverse fibres, but become arrested within the longitudinal fibre bundles. On progressing into the longitudinal bundles, the weak fibre/matrix interfaces allow the crack faces to be bridged by intact fibres. In turn, creep of the bridging fibres govern the rates of crack growth. Support for this view is then provided by the patterns of behaviour shown in Figures 1a and b, from which it can be shown that the times to fracture increase systematically with decreasing minimum creep rate. This creep rate dependence of the rupture life confirms that, since the longitudinal fibres control creep strain accumulation, these fibres also determine crack growth rates. However, the bridging fibres fail progressively as oxygen penetrates into the testpieces during creep exposure. As a result, the fracture surfaces of broken specimens show planar crack growth zones, characterized by in-plane oxidation-assisted fibre failure, together with regions where sudden failure occurs by fibre full out (Figure 3b). Yet, while this sequence of events is applicable to the four CMCs described in Table 1, differences in the susceptibility of the fibres to oxidation-assisted failure affect the observed creep ductility values.
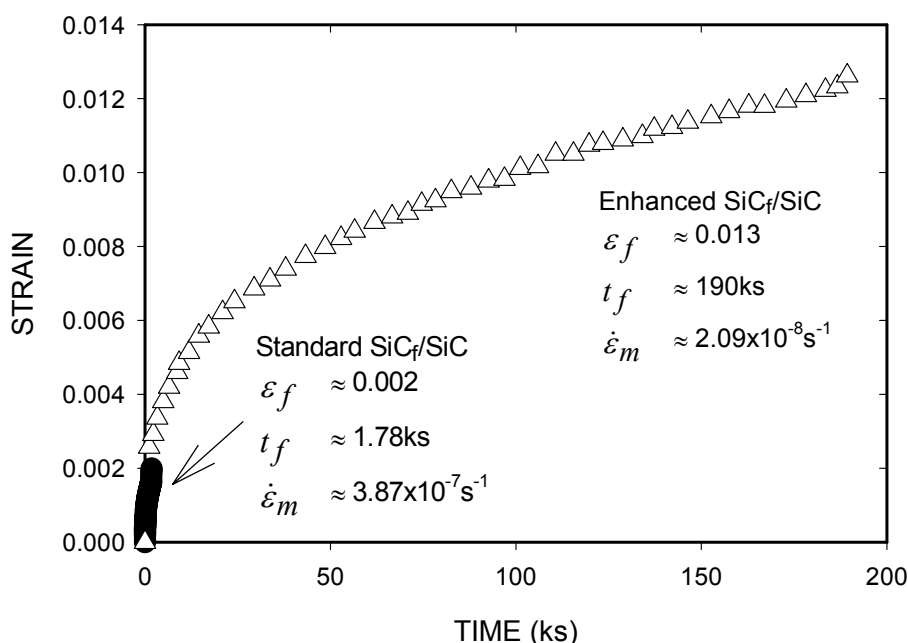
Figure 2. Creep strain/time curves at 90MPa for standard SiC$_f$/SiC and enhanced SiC$_f$/SiC at 1573K.
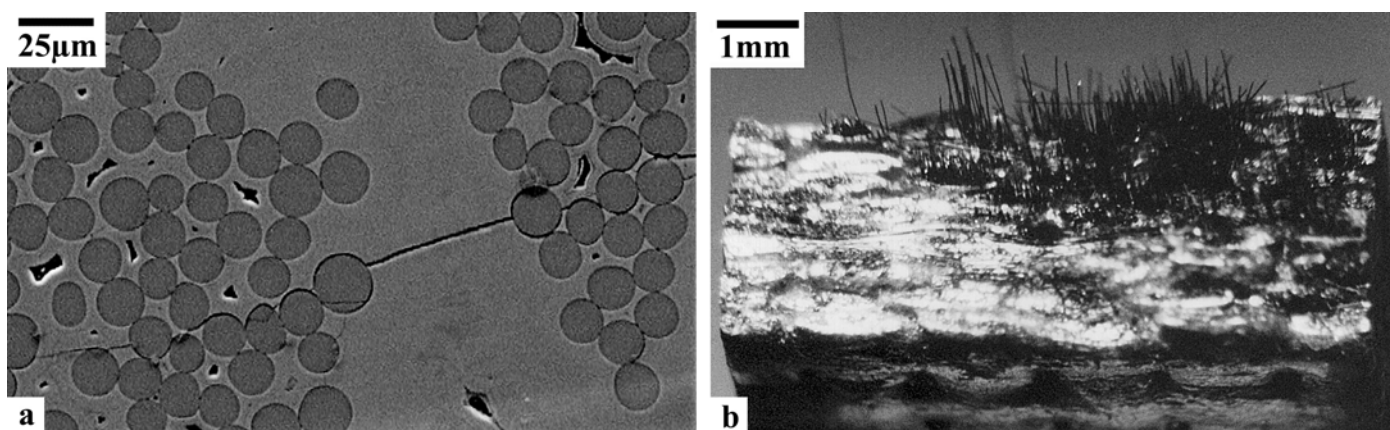
Figure 3. Micrographs showing (a) matrix cracking and (b) the planar crack growth zone and final fibre pull-out region on the fracture surface of a standard SiC$_f$/SiC sample.

With the standard SiC_f/SiC samples, cracks nucleate at macropores present in the matrix regions between the interwoven fibre bundles. These surface-nucleated cracks link up and grow, with oxygen penetrating directly along the opening crack. Rapid oxidation-assisted fibre failure then results in high crack growth rates, with low-ductility failure occurring when the cracks reach the size required to cause sudden failure by fibre pull out (Figure 3b). In contrast, with the enhanced SiC_f/SiC and $HNSiC_f/SiC$ materials, the glass-forming boron-based particles in the 'enhanced' matrices reduce the rates of oxygen penetration, oxidation-assisted fibre failure and crack growth. Consequently, creep must continue for longer times to reach higher strains (Figure 2) before the cracks attain the size needed for failure by fibre pull out.

With the SiC_f/Al_2O_3 composite, low rates of oxidation-assisted fibre failure also occur, but for different reasons. Firstly, residual-stress-induced microcracks present in the as-processed matrix [20] allow easy nucleation of many small cracks throughout the specimen gauge length, seemingly with oxygen ingress being relatively slow through the microcracked Al_2O_3 matrix. Secondly, the double BN/SiC interface layers are more resistant to oxidation than the carbon interfaces in the SiC_f/SiC type materials (Table 1). Hence, crack growth rates are lower and the creep ductilities are higher, resulting in creep rates and rupture lives comparable with those observed for the enhanced SiC_f/SiC and $HNSiC_f/SiC$ products (Figure 1).

Factors Affecting Creep Performance

The present analysis indicates several avenues for enhancement of the creep and creep fracture properties of fibre-reinforced CMCs. In particular, the longitudinal fibres control the rates of creep strain accumulation and crack growth, demonstrating that the development of new high-strength high-stability fibres of weaveable diameter (~15μm) is essential for future high-performance composites. Indeed, the data included in Figure 1a show that sintered silicon carbide displays creep strengths at 1773K [19] which match those of Nicalon™ NLM 202 fibres at 1573K, illustrating the potential for property improvement attainable with SiC fibres.

In this context, it is surprising that the creep properties of the $HNSiC_f/SiC$ samples produced with satin-woven bundles of Hi-Nicalon™ fibres are similar to those for the enhanced SiC_f/SiC product manufactured with plain-woven bundles of standard Nicalon™ fibres (Figure 1). However, the longest test reported for these materials lasted only ~100 hours [5,6], suggesting that long-term results are needed to quantify the benefits of incorporating satin-woven arrays of Hi-Nicalon™ fibres. Even so, the use of Hi-Nicalon™ fibres should offer advantages when double BN/SiC fibre/matrix interfaces are employed (Table 1). The BN coatings are less susceptible to oxidation than carbon interfaces [21,22], but the BN coating process [23] involves a high temperature treatment (> 1773K). Hi-Nicalon™ fibres should then avoid the property degradation expected with standard Nicalon™ fibres. Thus, recent studies have shown that no reduction in room-temperature strength of $HNSiC_f/SiC$ samples produced with 0.4μm thick BN interface layers occurred after exposure in air for 600h at 1673K, whereas significant strength reductions were found after 200h at 1273K with $HNSiC_f/SiC$ specimens manufactured with carbon interfaces [24].

While the matrices of the present SiC-fibre-reinforced CMCs contribute little to the overall creep strengths, the matrix compositions and microstructures affect the observed creep ductilities. Thus, the fracture modes exhibited by the standard SiC_f/SiC product indicate that the procedures adopted for densification of the fibre preforms must avoid the formation of macropores between the interwoven fibre bundles and large pores within the fibre bundles, which offer preferred sites for crack nucleation. Moreover, the matrices determine the rates of oxygen penetration into the composites during creep exposure, influencing the rates of oxidation-assisted failure of the crack-bridging fibres and the rates of crack growth. In this context, procedures such as the incorporation of boron-based particulate additives [16,17] are effective, resulting in the enhanced SiC_f/SiC and $HNSiC_f/SiC$ displaying creep and creep fracture properties substantially better than those found for the standard SiC_f/SiC samples (Figure 1). A further option could then be to employ surface coatings, just as the use of protective ceramic coatings extends the operational life of aeroengine turbine blades produced from nickel-base superalloys.

CONCLUSIONS

In contrast to the views expressed in earlier studies [4,5], the creep strengths of the reinforcing fibres exceed those of the matrices in SiC_f/SiC type materials, as proposed for the SiC_f/Al_2O_3 composite [7]. For the four SiC-fibre-reinforced CMCs considered (Table 1), the rates of creep strain accumulation are then controlled by the longitudinal fibres, with creep of the fibres accompanied by cracking of the weak porous matrices (Figure 3a). However, the creep strengths of individual fibres vary, as evident from the scatter in the data for Nicalon™ NLM 202 fibres (Figure 1a). Since the weakest fibre regions deform most easily, the creep rate decays with time as the stress is transferred to stronger fibres (Figure 2).

The rates of crack growth are also governed by the creep resistance of the longitudinal fibres which bridge the cracks developing through the longitudinal fibre bundles. Even so, oxygen penetration into the testpieces during creep exposure promotes oxidation-assisted failure of the crack-bridging fibres, affecting the creep strains at which fracture finally occurs by fibre pull out (Figure 3b). Fracture then terminates the decaying creep curves (Figure 2), with the creep ductility values influencing the minimum creep rates and rupture lives recorded (Figure 1). On this basis, the development of improved CMCs depends not only on the fibre reinforcement but also on the rates at which the matrices allow oxygen ingress and the susceptibility of the fibre/matrix interfaces to oxidation.

REFERENCES

[1]   Wilshire, B. and Carreño, F. (1999) *Mater. Sci. Eng*. A272, 38
[2]   Holmes, J. W. and Chermant, J.L (1993) In: *Proc. 6th European Conf on Composite Materials*, pp 633-647, Naslain, R., Lamon, J. and Doumeingts, D. (Eds). Bordeaux, France.
[3]   Lamouroux, F., Steen, M. and Vallés, J.L. (1996) *Comp. Sci. Tech*. 56, 825.
[4]   Zhu, S., Mizuno, M., Kagawa, Y., Cao, J., Nagano, Y. and Kaya, H. (1997), *Mater. Sci. Eng*. A225, 69.
[5]   Zhu, S., Mizuno, M., Nagano, Y., Cao, J., Kagawa, Y. and Kaya, H. (1998), *J. Am. Ceram. Soc*. 81, 2269.
[6]   Zhu, S., Mizuno, M., Nagano, Y., Cao, J., Kagawa, Y. and Kaya, H. (1999), *J. Am. Ceram. Soc*. 82, 117.
[7]   Wilshire, B. and Carreño, F. (2000) *J. Eur. Ceram. Soc*. 20, 463.
[8]   Prewo, K. M. (1986) *J. Mater. Sci*. 21, 3590.
[9]   Brennan, J. J. (1986) *Mater. Sci. Res*. 20, 546
[10]   Evans, A. G. and Marshall, B. D. (1989) *Acta Metall*. 37, 2657.
[11]   DiCarlo, J. A. (1994) *Comp. Sci. Tech*. 51, 213.
[12]   Bodet, R., Bourrat, X., Lamon, J. and Naslain, R. (1995) *J. Mater. Sci*. 30, 661.
[13]   Chollon, G., Pailler, R., Naslain, R. and Olry, P. (1995) In: *High-Temperature Ceramic-Matrix Composites II: Manufacturing and Materials Development*. pp299–236, Evans, A.G. and Naslain, R (Eds). Amer. Ceram. Soc., Westerville, OH.
[14]   Newkirk, M. S., Urquhart, A. W., Zwicker, H. R. and Breval, J. (1986) *J. Mater. Res*. 1, 81.
[15]   Newkirk, M. S., Lesher, H. D., White, D. R., Kennedy, C. R. and Urquhart, A. W. (1987) *Ceram. Eng. Sci. Proc*. 8, 879.
[16]   Elahi, M., Liao, K., Reifsnider, K. and Dunyak, T. (1995) *Ceram. Eng. Sci. Proc*. 16, 75.
[17]   Fox, D. S., (1995) *Ceram. Eng. Sci. Proc*. 16, 877.
[18]   Simon, G. and Bunsell, A. R. (1984) *J. Mater. Sci*. 19, 3670.
[19]   Wilshire, B. and Jiang, H. (1994) *Brit. Ceram. Soc*. 93, 213.
[20]   Heredia, F. E., Evans, A. G. and Andersson, C. A. (1995) *J. Am. Ceram. Soc*. 78, 2790.
[21]   Prouhet, S., Camus, G., Labrugere, C., Guette, A. and Martin, E. (1994) *J. Am. Ceram. Soc*. 77, 649.
[22]   Gonczy, S. T., Butler, E. P., Khasqiwale, N. R. and Tsakalakos, L. (1995) *Ceram. Eng. Sci. Proc*. 16, 433
[23]   Moore, A. W., Sayier, H., Farmer, S. C. and Morscher, G. N. (1995) *Ceram. Eng. Sci. Proc*. 16, 37.
[24]   Takeda, M., Imai, Y., Kagawa, Y. and Guo, S. Q. (2000) *Mater. Sci. Eng*. A286, 312.